Transient CFD Simulations of Wood Stoves with Varying Heat Storage Capacity

Mette Bugge*, Nils E. L. Haugen, Øyvind Skreiberg

Thermal Energy Department, SINTEF Energy Research, Trondheim, Norway
 mette.bugge@sintef.no

In the present work, transient CFD simulations of full wood log combustion cycles have been performed to study the time dependent behavior in cast iron and soapstone wood stoves. A model for the gas release is developed and implemented. The gas release model takes into account that the fuel gas release is transient, where both mass flow rate and gas composition as well as gas temperature changes with time. The effect of the wood stove material and its thermal inertia and conductivity on the combustion process and the transient heat release to the surroundings has been studied. In addition, transient variation in gas and wall temperatures as well as the combustion performance, was also studied. The simulations clearly show the effect of stove type on the transient heat release, which is controlled by the outer wall temperatures and the amount of heat transferred into the walls and their heat storage capacity. Due to the long real time duration of a full combustion cycle, these simulations are computationally very expensive and therefore only two-dimensional simulations were performed. The results show that the cast iron stove has higher outer wall temperatures and heat release during the combustion cycle than the soapstone stove. The soapstone stove has flatter profiles for outer wall temperatures and heat release to the surroundings and have a longer heat release period after the combustion cycle has ended.

1. Introduction

Combustion of wood logs in wood stoves and fireplaces occurs through a so-called batch combustion process, which is a highly transient process where most process parameters change during the combustion cycle. The batch combustion principle creates challenges with respect to both combustion control, efficiencies, emissions and heating comfort (Skreiberg and Seljeskog, 2018). During the initial phase of the batch cycle the moisture is evaporated, this is followed by the devolatilization phase and finally the char burnout phase. This means that the release of volatiles from the wood log is time dependent with respect to mass flow rate and gas composition, and the combustion conditions in the gas phase will change, which results in a varying heat production during the combustion cycle.

Heat is released from the outer stove walls to the surroundings through convection and radiation. The heat release to the surroundings is affected by the heat production during the combustion cycle, as well as the heat storage capacity (thermal inertia) and the conductivity and thickness of the wood stove walls, in addition to the initial wall temperatures. For a cast iron stove, the heat release to the surroundings during the combustion cycle will normally vary significantly due to the natural variation in heat production and the high thermal conductivity of the cast iron, giving a relatively small temperature difference across the wall and hence a faster heat release to the room. However, due to thermal comfort requirements, the heat release to the surroundings should be as stable as possible. The heat release profile can be flattened by improving the combustion process (more stable heat production), or the heat storage (higher thermal inertia) and transfer (lower thermal conductivity, lower density material). Using soapstone and in an amount giving a higher heat storage capacity (higher thermal inertia) instead of cast iron is one common option.

The objective of this work was to study the influence of varying stove heat storage capacity on the combustion process and the heat release to room using transient Computational Fluid Dynamics (CFD) simulations. The final goal would be to be able to utilize CFD as an efficient and reliable design tool for wood stoves, ensuring

cost-effective development processes resulting in high efficiency and low emission wood stoves providing the proper heating comfort required by the energy-efficient residential building stock of the future.

2. Methods

A commercially available 5 kW natural draught wood stove is used in this work. The wood stove has a combustion chamber volume resulting in a dry wood batch amount of 2 kg according to NS 3058 (1994). The mean wood consumption was set to 1.5 kg/h of dry wood, giving a combustion cycle duration of 80 minutes. The stove has both ignition, secondary and flushing air, where the ignition air should be closed after a few minutes. The secondary air is the air flowing through the row of air inlet holes in the upper back of the combustion chamber, while the flushing air is flowing through a slit in the upper front of the combustion chamber. The flushing air, which achieves the highest air preheating temperature, flows down along the stove glass, and serves to keep this clean. After the flushing air has passed the glass, it turns towards the woodpile, serving as primary air. ANSYS Fluent software (v16.2) was used in this work to carry out CFD simulations. A three-dimensional (3D) model of the stove was made (Figure 1, left), primarily for steady state simulations, while for transient simulations a two-dimensional (2D) model was developed (Figure 1, right). As a simplification, the glass was treated as a wall in the models. The 2D simulations were verified against the 3D model. To account for heat storage in the simulations the solid walls are included and meshed, using 53 000 elements in the entire 2D model. Heat release from the outer stove walls to the surroundings are accounted for through convection and radiation. The CFD simulations were performed using the k-ε realizable turbulence model and the Eddy Dissipation Concept (EDC) by Magnussen (Gran and Magnussen, 1996; Ertesvåg and Magnussen, 2000) for turbulent combustion in conjunction with the two-step CH_4 mechanism proposed by Westbrook and Dryer (1981). For radiation, the Discrete Ordinate model was used (Chui and Raithby, 1993).
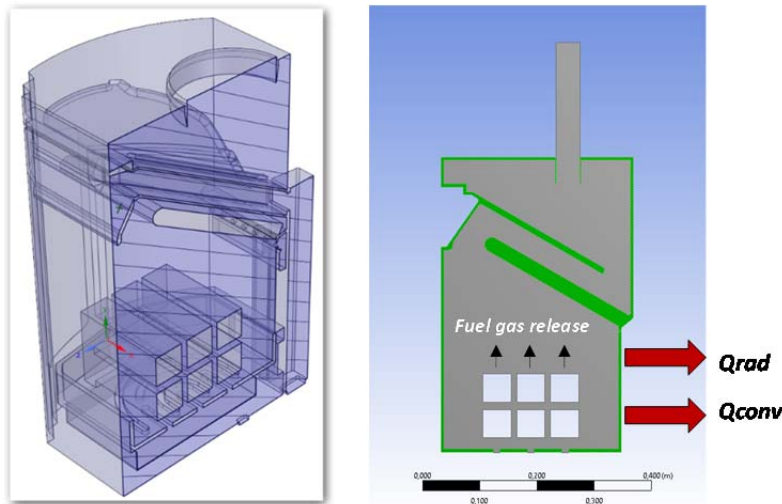

Figure 1: The 3D and 2D stove models.

Solid fuel conversion is not included in the CFD simulations, and the fuel gas is released from the outer surfaces of the woodpile. The fuel gas release is transient (drying, pyrolysis, char gasification) and the release is precomputed using an in-house transient model for the batch combustion process, ensuring element, mass and energy balance throughout the wood combustion cycle. Both mass flow rate, gas composition and gas temperature changes with time. In the CFD simulations, which starts from a cold stove, a transient fuel gas release and ignition is applied. The upper middle log in the woodpile is ignited first and during the first 2 minutes the fuel gas is released only from the middle log. After 2 minutes the front wood log is ignited and until 4 minutes fuel gas is released from both the front and middle log, while from 4 minutes the back wood log is ignited and fuel gas is released from all three upper logs. All the fuel gas is released from the top surfaces of the upper layer of wood logs, which is a justifiable simplification in this transient modelling approach. Figure 2 (left) shows the fuel gas (simplified to CO, CO_2, CH_4, H_2O) composition during the transient combustion cycle, while Figure 2 (right) shows the fuel gas flow rate and its temperature during the transient combustion cycle. As the combustion process proceeds, the char that is formed during the devolatilization process is gasified to CO, which enters the gas phase computational domain.
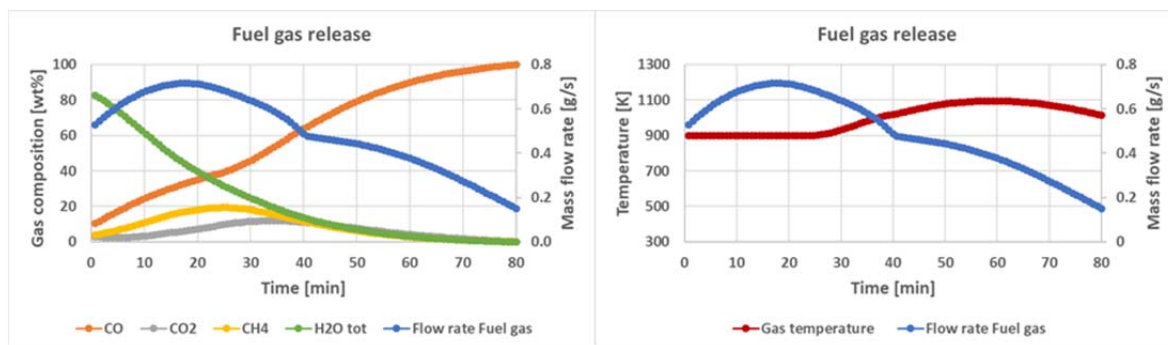
Figure 2: Fuel gas composition, flow rate and temperature.

The transient air flow rate is shown in Figure 3 (left) and is compared with the theoretical need, and the resulting transient excess air ratio is also shown. The transient air distribution between the three air inlets is shown in Figure 3 (right). The airflow distribution is based on 3D simulations when applying a draught of 10 Pa. The airflow distribution from the 3D simulations has been validated against experimental results. Ignition air is closed after 5 minutes. In the transient CFD simulations, flushing and secondary air have been kept constant between 80 and 120 minutes, i.e. after the combustion cycle has ended, and they were closed at 120 minutes. The simulations were continued for 60 minutes after the air valve was closed, until 180 minutes. The temperatures of the inlet air during the combustion cycle (until 80 minutes) was set constant to 373, 373 and 673 K for the ignition, secondary and flushing air, respectively. After the end of the combustion cycle and until 120 minutes, a 50% linear reduction of the secondary and flushing air temperatures compared to the ambient temperature were applied for the cast iron stove, while a 25% linear reduction was applied for the soapstone stove.
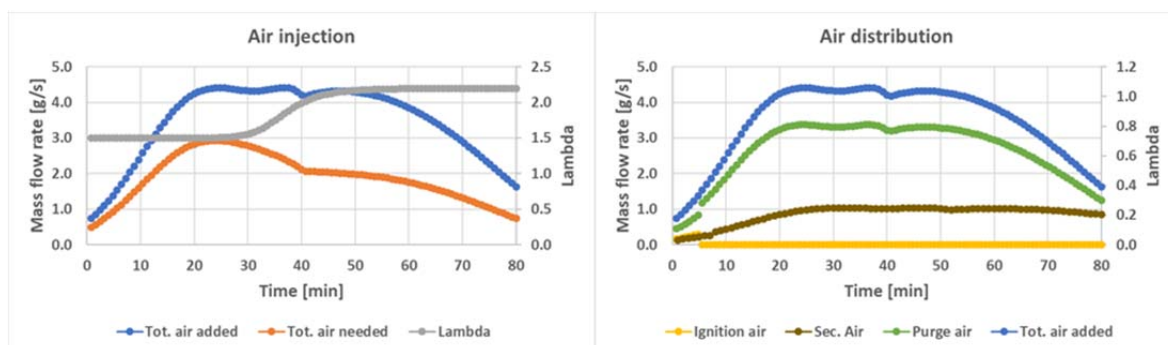

Figure 3: Air flow rate and distribution, and excess air ratio.

3. Results and discussions

Transient simulations were performed for a full wood combustion cycle in a cast iron stove with 5 mm cast iron walls included and meshed. Transient boundary conditions were applied, where the fuel gas release and air injection changes with time. From the simulations, relevant time dependent parameters such as temperatures, gas compositions and heat release during the combustion cycle and after the combustion cycle ends can be extracted. Figure 4 shows different temperatures throughout the combustion cycle for the cast iron stove. Tmean is the mean gas temperature in the combustion chamber, Tout is the mean flue gas exit temperature, Twall is the mean outer walls temperature, while Tw_backlow and Tw_frontlow are the mean outer wall temperatures of the lower back wall and lower front wall, respectively. As expected, the temperature of the front wall is significantly higher than the temperature of the rear wall, as the combustion process is more intense, and the gas phase temperatures are higher in this region. Included in Figure 4 is also the stove temperatures at two instances in time, after 6 and 50 minutes. After 6 minutes, fuel gas is released from the top surface of all three upper wood logs, however, the stove temperatures are low. After 50 minutes the combustion process is well established, and much higher stove temperatures can be observed. As can be seen in Figure 4, a significant increase in gas temperatures occurs after about 6 minutes. There are large variations in temperatures during the combustion cycle, and a noticeable change when the combustion cycle ends, also for wall temperatures. Also the heat release to the surroundings varies during the combustion cycle. As the different walls are exposed to different heat load, giving e.g. higher temperature for the front wall

than the back wall, the heat release to the surroundings from the respective outer walls are influenced accordingly. When looking at the gas composition, some unburned CO/CH$_4$ can be found at the flue gas exit, which indicates that the combustion is not complete.
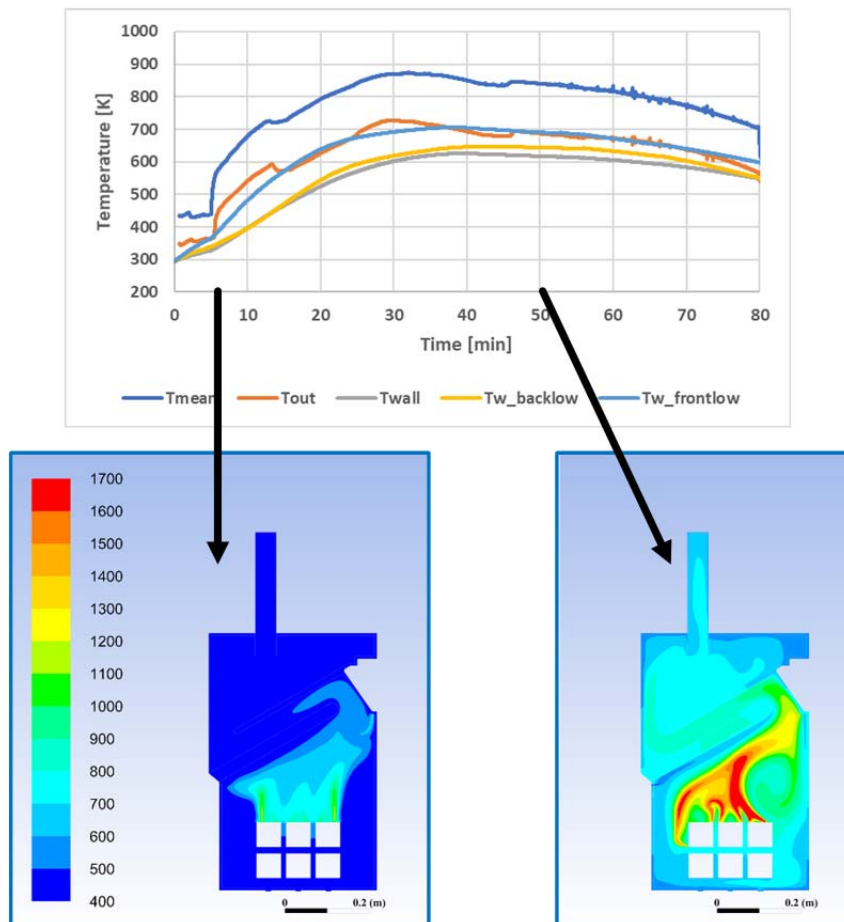

Figure 4: Calculated fluid and wall temperatures.

In Figure 5, the temperatures for the cast iron stove are shown together with the normalised heat release profile (Qnorm) to the surroundings. This is shown from the beginning of the combustion process until 40 minutes after the combustion cycle has ended. A heat release profile to the surroundings with a distinct heat release peak can be seen. A distinct drop in the mean gas temperature in the combustion chamber and the flue gas exit temperature can be seen when the combustion cycle ends after 80 minutes, and thereafter a continuous decrease in all temperatures can be seen. In Figure 6 the stove temperatures are shown at selected instances in time, showing the evolution of the combustion process, from 5 to 70 minutes.
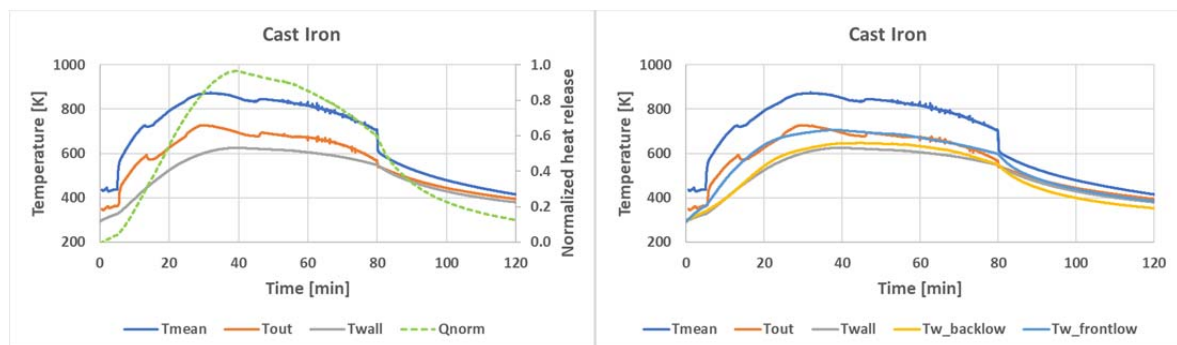

Figure 5: Fluid and outer wall temperatures, and heat release profile for the cast iron stove. Normalized heat release is related to "(nearly) maximum" heat release.
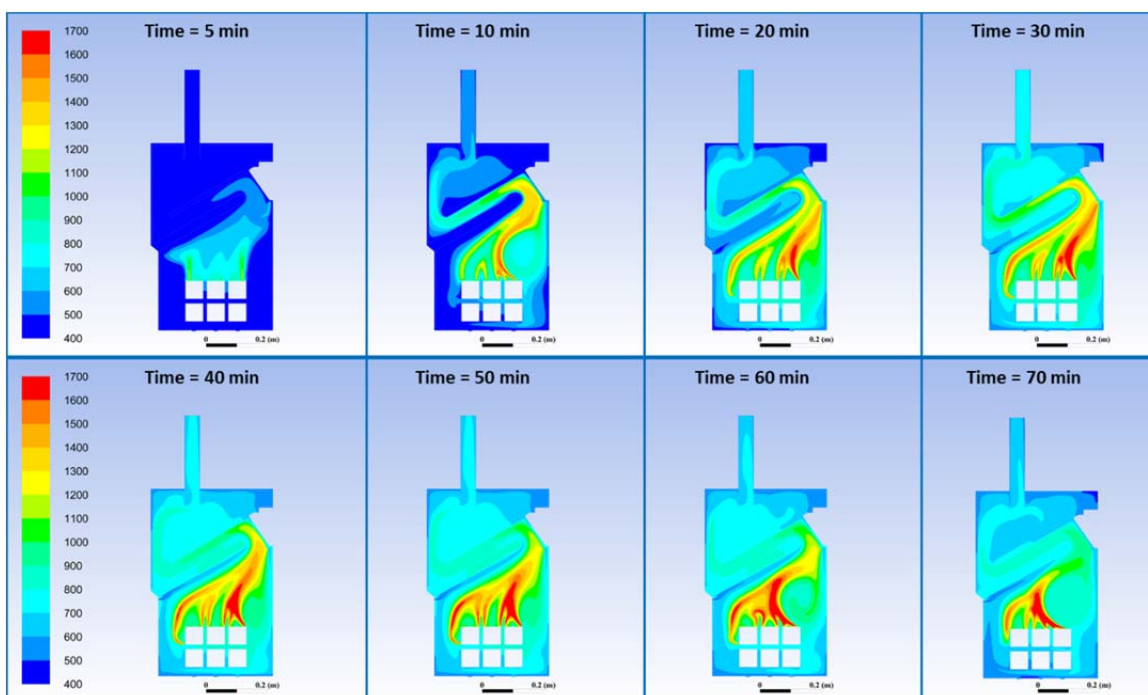
Figure 6: The stove temperatures at selected instances in time.

To compare with a heat storage stove, the cast iron was replaced with 50 mm soapstone. All other simulation parameters were kept the same as in the cast iron case. As expected, a significant increase in the gas temperatures after about 6 minutes can be seen (Figure 7), as well as variations in temperatures during the combustion cycle. However, the mean gas temperature in the combustion chamber, and at the flue gas exit, are lower than for the cast iron stove. Also, a flattened profile for the outer wall temperatures can be seen. This results in a relatively flat heat release profile to the surroundings. Some more unburned CO/CH$_4$ was found at the flue gas exit compared to the cast iron stove, indicating somewhat poorer combustion performance. This can be expected based on the lower mean gas temperature in the combustion chamber.
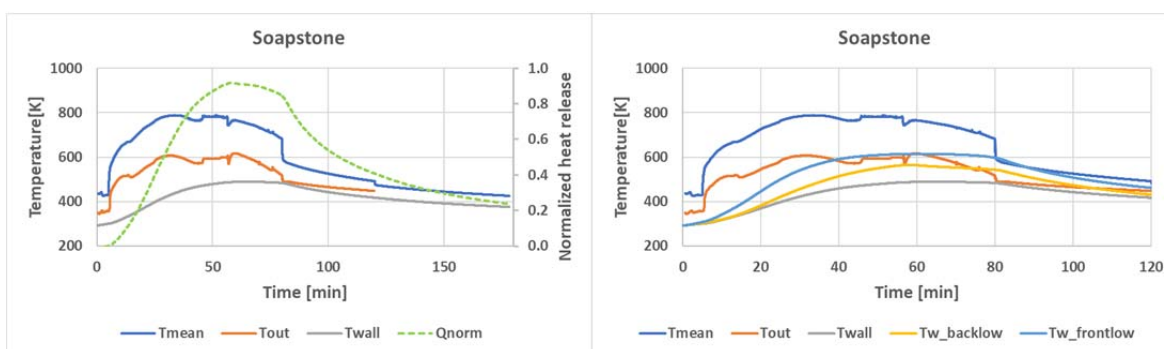

Figure 7: Wall temperatures and heat release profile for the soapstone stove. Normalized heat release is related to "(nearly) maximum" heat release.

In Figure 8 the results from the cast iron and soapstone cases are directly compared, clearly showing the flattened heat release profile to the surroundings for the soapstone stove compared to the cast iron stove. This is a result of the lower outer wall temperatures for the soapstone stove, which again is a result of the higher heat storage capacity/thermal inertia and lower conductivity of the soapstone. As a result, the soapstone stove stores more heat, which is released for a much longer time after the combustion cycle has ended.
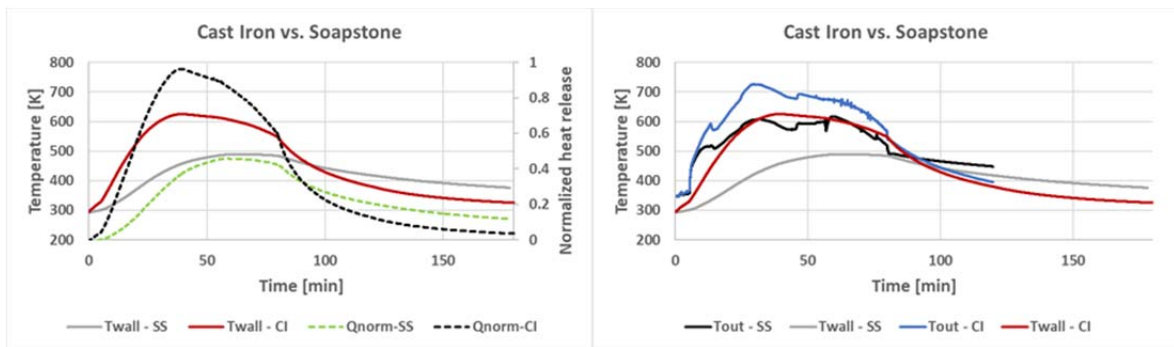
Figure 8: Results from the cast iron and soapstone cases directly compared. SS = Soapstone. CI = Cast iron.

Similar results have been shown earlier by Skreiberg and Georges (2017) using a simplified modelling approach where a heat production profile has been forced through cast iron and soapstone stove walls. A main advantage of CFD simulations is the transient calculation of the heat transferred through the wall, as well as the flue gas exit temperature. The ultimate approach would be a directly coupled solid fuel and gas phase computational domain, where only initial conditions are defined, and all other variables are calculated throughout the transient combustion cycle (i.e.; where the gas release from the wood logs is directly controlled by the heat load from the gas phase and the corresponding heat transport through the wood). This is planned future work.

4. Conclusions

Transient simulations have been performed for a full wood combustion cycle, including a period after the combustion process has ended. The effect of varying heat storage has been studied through transient simulations. The wood stove heat storage capacity/thermal inertia affects the heat release to the surroundings as expected, and the wood stove heat storage also affects the combustion process. The cast iron stove has higher outer wall temperatures and heat release during the combustion cycle than the soapstone stove. The soapstone stove has more flattened profiles for outer wall temperatures and heat release to the surroundings and have a longer heat release period after the combustion cycle has ended. From the simulations, a comprehensive amount of data is available for the entire combustion cycle. Based on the transient simulation results, instances to be investigated in detail in steady state CFD simulations can be identified, as well as boundary conditions for these steady state simulations. Heat transfer profiles from the simulations can be used as input in parametric studies using other tools/methods, e.g. to assess thermal comfort in buildings equipped with wood stoves. The new modelling approach developed can be further developed to study combustion and energetic efficiency as well as emissions in more detail. A validated directly coupled solid fuel and gas phase computational domain would be the ultimate approach.

References

Chui E.H., Raithby G.D., 1993, Computation of radiant heat transfer on a nonorthogonal mesh using the finite-volume method, Numerical Heat Transfer, Part B., 23, 269-288.

Ertesvåg I., Magnussen B.F., 2000, The Eddy Dissipation turbulence energy cascade model, Comb. Sci. Technol., 159, 213-236.

Gran I., Magnussen B.F., 1996, A Numerical Study of a Bluff-Body Stabilized Diffusion Flame. Part 2. Influence of Combustion Modeling and Finite-Rate Chemistry, Comb. Sci. Technol., 119, 191-217.

NS 3058, 1994, Enclosed wood heaters, Smoke emission.

Skreiberg Ø., Georges L., 2017, Wood stove material configurations for increased thermal comfort, Energy Procedia, 142, 488-494.

Skreiberg Ø., Seljeskog M., 2018, Performance history and further improvement potential for wood stoves, Chemical Engineering Transactions, 65, 199-204.

Westbrook C.K., Dryer F.L., 1981, Simplified reaction mechanism for the oxidation of hydrocarbon fuels in flames, Comb. Sci. Technol., 27, 31-43.